

Real-time Adaptive Approach for Hidden Targets Shape Identification using through Wall Imaging System

Sandeep Kaushal[#], Bambam Kumar[@], Prabhat Sharma^{\$}, and Dharmendra Singh^{*}

[#]*Department of Electronics and Communication Engineering, ACET, Amritsar - 143 109, India*

[@]*Department of Electronics and Communication Engineering, National Institute of Technology, Patna - 800 005, India*

^{\$}*Instrument Research and Development Establishment, Dehradun - 248 008, India*

^{*}*Department of Electronics and Communication Engineering, Indian Institute of Technology, Roorkee - 247 667, India*

**E-mail: dharmfec@iitr.ernet.in*

ABSTRACT

In Through-wall Imaging (TWI) system, shape-based identification of the hidden target behind the wall made of any dielectric material like brick, cement, concrete, dry plywood, plastic and Teflon, etc. is one of the most challenging tasks. However, it is very important to understand that the performance of TWI systems is limited by the presence of clutter due to the wall and also transmitted frequency range. Therefore, the quality of obtained image is blurred and very difficult to identify the shape of targets. In the present paper, a shape-based image identification technique with the help of a neural network and curve-fitting approach is proposed to overcome the limitation of existing techniques. A real time experimental analysis of TWI has been carried out using the TWI radar system to collect and process the data, with and without targets. The collected data is trained by a neural network for shape identification of targets behind the wall in any orientation and then threshold by a curve-fitting method for smoothing the background. The neural network has been used to train the noisy data i.e. raw data and noise free data i.e. pre-processed data. The shape of hidden targets is identified by using the curve fitting method with the help of trained neural network data and real time data. The results obtained by the developed technique are promising for target identification at any orientation.

Keywords: TWI; Neural network; Threshold; Curve-fitting

1. INTRODUCTION

Through-wall imaging detection and identification are one of the most challenging tasks for military applications, surveillance and security of the public and their assets because hidden targets cannot be sensed through conventional techniques. In this domain of these applications, a key challenge for these applications is not only to find the presence of various targets behind the wall but also to identify their shape and size. Researchers have implemented ultra-wideband microwave imaging radar, based on the stepped frequency mode, to penetrate through concrete wall materials and make smart decisions about the contents of buildings, but still trying to develop some intelligence techniques to identify the hidden objects. Nevertheless, the deep machine learning and soft computing methods have been used to classify the targets in different domain applications^{1,2}. As a microwave imaging radar based on the stepped frequency continuous wave (SFCW) technique is commonly applied to various practical applications including civil engineering^{3,4}, detection of pipes and cables buried in the ground^{5,6}, through-wall radar imaging⁷⁻¹¹, medical imaging¹², feature estimation of the road surface layer¹³, and many applications of ground penetrating radar (GPR)¹⁴⁻¹⁷.

SFCW radar also has various advantages such as, high receiver sensitivity and high mean transmitter power. It does not only offer good capability of detecting the targets but also improves range accuracy, facilitates clutter rejection, and helps in suppressing the multipath propagation⁷.

In recent years, many artificial intelligence problems have been solved using convolutional neural networks (CNNs). CNN offers a lot of advantages over the other machine learning methods in resolving complicated learning tasks. In conventional identification methodologies, various features such as colours, edges and corners are physically extracted and designed and after that support vector machine (SVM) techniques are used as traditional classifier^{18, 19}.

In literature, through-wall imaging system has been classified into two categories: one is based on image detection and the other is on feature extraction. The first category uses the beam focusing algorithms such as back projection, delay and sum, etc. The beam focusing parameter, an accurate wall characteristic estimation, is one of the main challenges of through-the-wall imaging (TWI) system. The propagation velocity of electromagnetic wave (EM) waves is affected by dielectric constant and thickness of the wall. Therefore, the wall parameters such as thickness and dielectric constant needs to be estimated precisely. A small error in the wall parameters

results in blurring of the target image and subsequently, declines signal-to-clutter ratio (SCR)^{20,21}. Hence, the quality of the image is not as good as per actual shape and size of the target. The second category offers to extract the significant features of the target such as movement characteristics^{22, 23}, vital signs²⁴ of the target and pole-extraction approach for the estimation of unknown parameters of a multi-layered wall²⁵. Although, the most important disadvantage of these methods is that, it can only find the presence or absence of targets. The shape of targets has been detected by using artificial neural network²⁶. In this paper, authors used a binary image for training the neural network. These types of techniques are suitable for regular shapes of targets but for complex-shaped targets such as dummy metal shape of a man, it is very difficult to generate a binary image. The shape of metallic cylinder targets has been detected by a dynamic differential evolution (DDE) stochastic searching algorithm but this technique is not suited for low dielectric targets such as wood and tiles due to low E-field scattering²⁷. A time-delay difference curve (TDDC) has been used to estimate the target's contour behind walls with known wall parameters using UWB-SP radar²⁸. The width of low dielectric targets such as Teflon has been detected by a low rank approximation method in which clutter reduction technique as singular value decomposition (SVD) is used to decompose the data into a low rank component i.e. largest Eigen value of image²⁹.

In this paper, a target database of various orientation for TWI has been used for ANN training for known wall parameters. The trained ANN data has been correlated with real time target data for shape identifying and the same trained data has been used to estimate the threshold by a curve fitting technique. Therefore, the proposed novel shape identification technique with fusion of artificial neural networks and real time TWI target data followed by curve fitting method and correlator has been used for the smart threshold decision of targets through the wall.

2. EXPERIMENTAL SET UP AND DATA COLLECTION

SFCW is a frequency-domain pulse synthesis method that has been applied to radar systems for data collection. In order to have full imaging information, the target is scanned in two orthogonal directions, i.e., horizontal (along the width) and vertical (along the height), to cover the target completely. This scanning method is called C-scan⁷⁻¹¹. C-Scan data is collected by moving TWI antenna in the horizontal direction at 30 different locations and, at 25 different vertical locations each with 5 cm step size, both in horizontal and vertical directions. The dimension of C-scan data is (201x30x25), where, 201 is the number of frequency points. C-scan provides valuable information about the complete shape of a target in terms of width and height. 2-D images (30x25) are generated from 3D C-scan data by taking the slice at particular range bin that is decided by the range profile of targets²⁶. The obtained images have been normalised and they are called raw images³⁰. Frequency range from 1 GHz to 3 GHz (BW=2 GHz) chosen for shape identification of the target. The range and cross-range resolution of SFCW radar are very important parameters to

distinguish between two closely spaced targets in down range and lateral directions, respectively^{26, 29}. The range resolution is ($\Delta Y = C/2P\Delta f = 7.5$ cm), where C is speed of EM wave, N is the number of frequency points and Δf is the frequency step size. The one port S-parameter, S11 was collected at P = 201 frequency points, i.e., frequency step size of 10 MHz ($\Delta f = BW/P = 10$ MHz). The distance between TWI system and the front side of the wall is 40 cm, thickness and the dielectric constant of the wall are 20 cm and 5.4, respectively and distance between the back side of the wall and target is 80 cm. The cross-range resolution ($\Delta X = \lambda R/D = 9.3$ cm) where λ is the minimum wavelength of transmitted signal, R is standoff distance between targets and TWI setup and D is the lateral dimension of synthetic aperture, i.e. (5 cm × 30 = 150 cm). The scanning step size should be less than the cross-range resolution³⁰.

A total of 120 samples are captured by the TWI system for the metal, wooden and tiles target of different shapes and size in different orientations as shown in Table 1. The strength of the collected samples depends on the target characteristics, like permittivity, shape, orientation, etc. The signal strength of a metallic target is stronger than the wooden and tile-based targets, because of its permittivity. The metallic rectangular, circular, triangular, dummy metal man, square wood and tile targets have been placed behind a 20 cm thick concrete wall and rotated from -45° to +45° at 5° rotation step-size. 19 readings have been taken by the single target; there are 6 targets so 114 readings have been obtained for targets behind the wall and the remaining 6 readings have been taken of the empty scene.

3. PROPOSED SCHEME

TWI data may be corrupted by clutter and noise, due to variation in wall characteristics and target characteristics. Clutter is interpreted by any unpredicted and uneven reflections, which can be presented in the collected TWI data, hence TWI interpretation is not an easier task. Behind the wall, metal sheet, wood, tiles, and the empty scene have been considered as the target for TWI experiment. The present paper is focused on shape identification of a subjected target by using ANN, curve intersection and correlation technique. Figure 1 describes the proposed scheme of shape identification for the experiment.

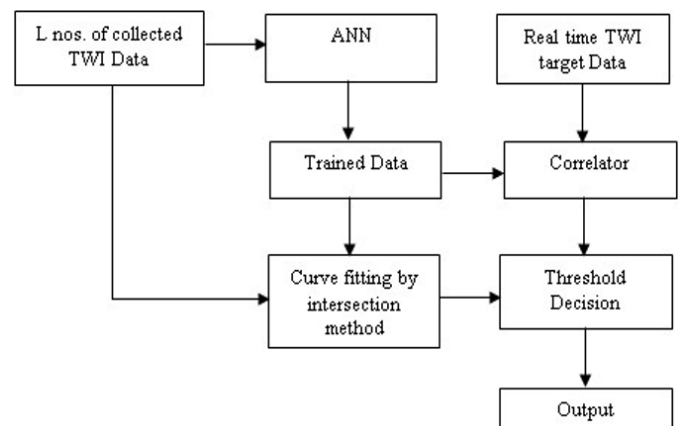









Figure 1. Proposed scheme of shape identification for TWI experiment.

Table 1. Description of targets with orientation and corresponding ID

S. No	Target	Target orientation	Target ID
1	 <p>Rectangular metal sheet 61cm x 55cm (length x breadth) and 3mm thick</p>	-45°, -40°, -35°, -30°, -25°, -20°, -15°, -10°, -5°, 0°, +5°, +10°, +15°, +20°, +25°, +30°, +35°, +40° and +45°	MRT1 to MRT19 MRT means Metal Rectangular Target
2	 <p>Diameter of circular metal sheet is 40.5 cm and 1mm thick</p>	-45°, -40°, -35°, -30°, -25°, -20°, -15°, -10°, -5°, 0°, +5°, +10°, +15°, +20°, +25°, +30°, +35°, +40° and +45°	MCT20 to MCT38 MCT means Metal Circular Target
3	 <p>Dimension of triangular metal sheet is 58.5 cm (length of each side) and 3mm thick</p>	-45°, -40°, -35°, -30°, -25°, -20°, -15°, -10°, -5°, 0°, +5°, +10°, +15°, +20°, +25°, +30°, +35°, +40° and +45°	MTT39 to MTT57 MTT means Metal Triangular Target
4	 <p>Square wood sheet 45cm x 45cm (length x breadth) and 5mm thick</p>	-45°, -40°, -35°, -30°, -25°, -20°, -15°, -10°, -5°, 0°, +5°, +10°, +15°, +20°, +25°, +30°, +35°, +40° and +45°	WST58 to WST76 WST means Wood Square Target
5	 <p>The dimension of Square Tile is 45 cm x 45 cm (length x breadth) and 10 mm thick</p>	-45°, -40°, -35°, -30°, -25°, -20°, -15°, -10°, -5°, 0°, +5°, +10°, +15°, +20°, +25°, +30°, +35°, +40° and +45°	TST77 to TST95 TST means Tiles Square Target
6.	 <p>Dummy metal man shape and its thickness is 3 mm</p>	-45°, -40°, -35°, -30°, -25°, -20°, -15°, -10°, -5°, 0°, +5°, +10°, +15°, +20°, +25°, +30°, +35°, +40° and +45°	DMT96 to DMT114 DMT means dummy Metal man Target
6	 <p>Empty Scene</p>		EST115 to EST120 EST means Empty Scene Target

The collected TWI data for various known and unknown targets has been trained by ANN. The trained data is correlated with real time TWI data. Output of correlator has been thresholded by a curve fitting intersection method. The detail of the method has been discussed in sub-section 3.2.

The overall developed scheme is summarised in the following steps:

- Random collection of L nos. of TWI data, whether target is present behind the wall or not.
- Trained collected data (noisy and noise free) by Artificial Neural Network (ANN) for least mean square error (MSE).
- As MSE is achieved then training will be stopped.
- Trained data and real time TWI target data will be correlated with each other.
- If the target is present, then some shaped target and clutter will be the result, otherwise only background image will be there.
- Curve fitting method is applied on randomly collected TWI data and on ANN trained data.
- The threshold is estimated by finding the intersection point of both data (TWI data and ANN data).
- The threshold decision removes the unnecessary noise data, resulting in image formation of the target and also its shape is identified

3.1 Data Organisation for Artificial Neural Network (ANN)

3 D C-scan data has been collected for the metallic, wooden, tiles and empty scene target of different shapes and size in different orientation and converted in 2D ($M \times N$) from 3D C-scan data by taking the slice at particular range bin that is decided by the range profile of targets²⁶. A total of 120 samples are captured by through-wall radar imaging system. Let TWI data is denoted by Z , which is noisy data and has the dimensions of $M \times N$. Here, M represents the number of horizontal scanning points and N represents the number of vertical scanning points for a specific target. If noise/clutter in TWI measurement represented by Y and noise free data represented by X . Let Y be the noise of dimensions of $M \times N$, if noise mix in TWI noise free data, i.e. X , which may be given as²⁹:

$$Z = X + Y \quad (1)$$

where Z represents the Noise mix TWI data or raw data, which also have the same dimension as X . There may be a possible noise, Y , correlated or uncorrelated with TWI data X . Consider Z data for a metal target, wood sheet target, tiles, and empty scene etc., i.e. the data should be considered for a variety of targets behind the wall. Collected data for various considered targets may be represented by the following equation:

$$L = \{Z_1, Z_2, Z_3, \dots, Z_n\} \quad (2)$$

where, L represents the set of collected data for n number of targets, which may also include the data of without any target.

The bunch of collected data L is given to the input of ANN. The structure of ANN is depicted in Figure 2, where L is considered as input data, which includes data of multiple kinds of targets. Each L data represents the node input to ANN. Output of each input node given as input to hidden layer node.

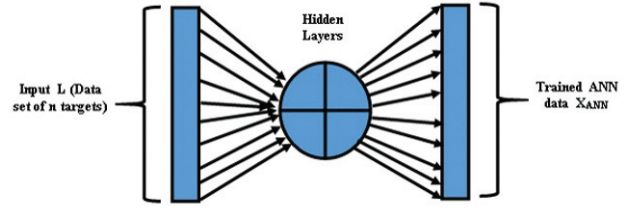


Figure 2. ANN Structure for TWI.

Hidden layers connect the input node and the final output node through a transfer function. After completion of the training as given in steps (i) to (iv) of section (3), ANN trained output data goes to output nodes.

For training of ANN, Noise free target data has been made by statistical analysis of measured noisy target data. Suppose measured noisy target data is represented by Z_{meas} . Applying data windowing, subtracting wall thickness, and finally apply background subtracting by using averaging technique, we get the noise free target data $X_{NFREE}^{26, 29-30}$. Rectangular windowing technique has been used to remove the antenna-air interference³⁰. The known wall parameters are used for velocity correction so that focused image can be obtained²⁹. The average subtraction method is used as background subtraction to remove the clutter as well as the noise of image²⁶. Mathematically, X_{NFREE} may be given by following equation:

$$X_{NFREE} = \text{Windowed}(Z_{meas}) - \text{wall parameters estimation} - \text{Average}(Z_{meas}) \quad (3)$$

Collectively, the bunch of X_{NFREE} may be represented by the following equation:

$$P = \{X_{NFREE 1}, X_{NFREE 2}, X_{NFREE 3}, \dots, X_{NFREE n}\} \quad (4)$$

where P represents the set of target's noise free data, which is used as reference input of ANN. ANN model consists the three stage such as the input stage, hidden layer stage, and output stage^{26,30}. The prime task is to identify the shape of targets through the concrete wall at any angle. To resolve such problem, six targets such as the metal rectangular sheet, metal circular sheet, metal triangular sheet, wood square sheet, tiles and the empty scene have been taken and rotated between -45° to $+45^\circ$, at every 5° behind the wall. Hence, data set of 120 samples are made with nineteen dissimilar rotation directions (-45° to $+45^\circ$) for six targets and six without target readings have been taken ($19 \times 6 + 6 = 120$). For identifying the shape of the target, 102 random selected data (85%) out of entire 120 samples data have been selected to train ANN model and for testing and for the validation of the trained neural network, the remaining 18 data (15%) has been considered²⁶. The input stage consists of (30×25 , 102) data sets, where the dimensions of the single image is (30×25) and total 102 such images have been considered to train the ANN model. To recognise the shape of targets behind the wall, a multilayer feed-forward neural network (MFFNN) is used which consists of a pattern recognition network with the sigmoid transfer function and scaled conjugate gradient (SCG) training function in both the output layer and hidden layer²⁶. In our proposed NN model, hidden layer consists of 50 neurons. The weight and bias value of hidden layer has been updated according to SCG function

and output of the network, which should be valued between 0 to 1, has been constrained by a sigmoid transfer function.

Before starting training through ANN, L and P set of data have been assigned as input (noisy data) and reference data (noise free) to train ANN, whose dimensions are (30×25, 102), respectively²⁶. To identify the shape of targets and making it rotation invariant, single reference data is assigned to all input data for the same type of target. For example, for metal rectangular targets, the same reference data that generated at 0° orientation has been assigned to all nineteen metal rectangular input data. Now train ANN and observed the variation in mean square error (MSE). When variation will be imperceptible, ANN is considered as trained for our reference target data set P .

3.2 Target Identification for TWI

Let trained ANN data is represented by X_{ANN} and real-time TWI data (i.e. not used for training ANN) for the considered target is represented by $Z_{realtime}$. The image has been obtained from real time data by taking the slice at a particular range bin of 3D C-scan data, which is shown in Fig. 3. As from Fig. 3, there is no clue about target shape and features of targets, therefore, correlated the X_{ANN} and $Z_{realtime}$ observe the results, shown in Fig. 4. Some target shape information is extracted after correlation, but few background noise components are still present in the image. So, there is a need to threshold the image with some means and filter out the background noise.

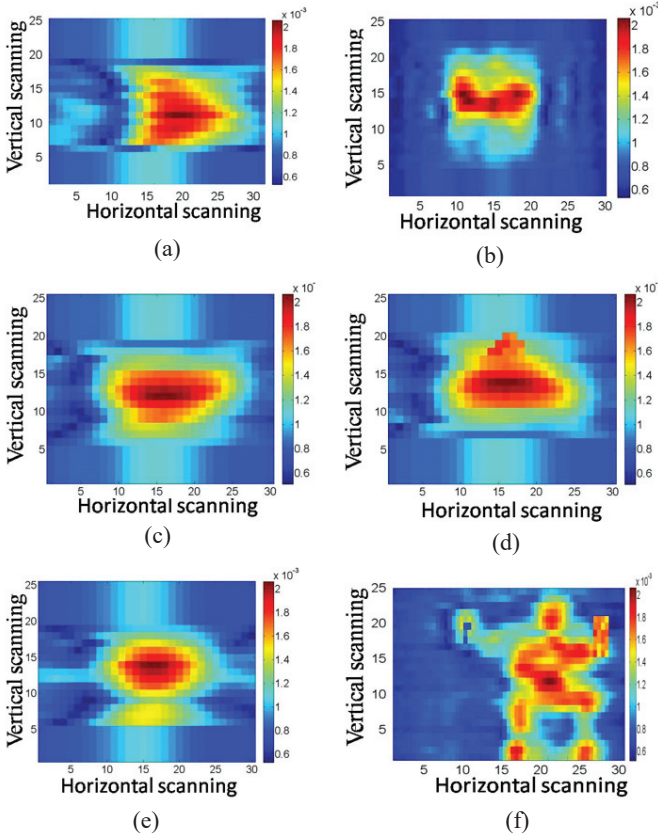


Figure 3. Raw image of (a) Metal Circular target (b) Metal rectangular target (c) Tiles target (d) Metal Triangular targets (e) Wood square target and (f) Dummy metal man target.

3.3 Threshold Decision

The threshold decision is required for filtering of the background noise component and clear identification of the target. For deciding the threshold, find the intersecting point between input data set P (from Eqn (4)) and ANN trained data X_{ANN} by curve fitting and root mean square error method³¹. Further, take the real time pre-processed (windowing, wall-parameter subtracting and averaging for subtracting the background) considered target data, which is represented by $X_{realtime}$. Now, both data X_{ANN} and $X_{realtime}$ fitted on polynomial, which is given by the following equation:

$$p(x) = p_1x^n + p_2x^{n-1} + p_3x^{n-2} + \dots + p_{n+1} \quad (5)$$

where, $p(x)$ is n^{th} order polynomial, p_1, p_2, \dots, p_{n+1} are its coefficients and x is input to polynomial. The coefficients of polynomial are obtained by the curve fitting approach on the basis of coefficient of determination (R^2) values which are greater than 0.9³¹⁻³².

We got two polynomial curves, one for X_{ANN} and another for $X_{realtime}$. Both fitted polynomial may intersect to each other, that intersecting point can find by difference of the fitted curve gives the intersection points for a root mean square error (RMSE). The final threshold value has been calculated by computing the ratio of the estimated threshold to measured threshold. The estimated threshold value is calculated with the help of X_{ANN} data set and measured threshold value is calculated

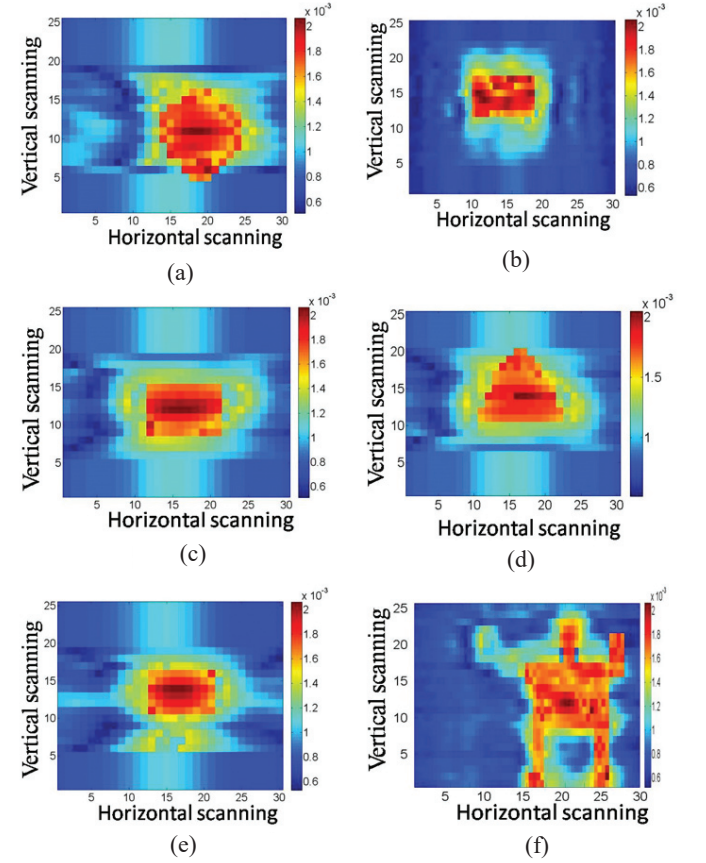


Figure 4. Trained ANN image of (a) Metal circular target (b) Metal rectangular target (c) Tile target (d) Metal Triangular targets (e) Wood square target and (f) Dummy metal man target.

with the help of $X_{realtime}$. The intersection of the curve has been shown in Figure 5. In Fig. 5, Y-axis represents the threshold for X_{ANN} and X-axis represents the threshold for $X_{realtime}$.

If both curves intersect at one common point, the threshold value may be calculated by following relation:

$$Threshold = \frac{Th_{ANN}}{Th_{meas}} \quad (6)$$

where, measured threshold by $X_{realtime}$ denotes as Th_{meas} and estimated threshold by X_{ANN} denotes as Th_{ANN} .

The curves may intersect at multiple points, the final threshold value calculation is tricky in this case. Let consider Fig. 5, where curves are intersected at two points, so threshold for Fig. 5 is given by the following relation:

$$Threshold_{multiple} = \frac{Th_{ANN \max} - Th_{ANN \min}}{Th_{meas \max} - Th_{meas \min}}$$

$$Threshold_{multiple} = \frac{0.02452 - 0.02435}{0.1995 - 0.0891} = \frac{0.00017}{0.1104} = 0.00154 \quad (7)$$

Once threshold has been decided by Eqn (7), it is applied on ANN trained images, as shown in Fig. 4. The obtained threshold images are shown in Fig. 6. Here, image intensity has been compared with the threshold. If it is less than the threshold, considered as background, otherwise, treated as target intensity. The final threshold images, which are shown in Fig. 6, are clearly visualising the target shapes by making smooth background as compare to Figs. 3 and 4. Hence, developed real-time target's shape identification methodology is promising.

The proposed technique is tested on various considered targets and its results are shown in Table 2. Targets ID MCT28, MTT51, TST88 and EST indicate the metal circular target at -5° orientation, the metal triangular target at 15° orientation, the tile target at 10° orientation and the empty scene, respectively. Therefore, the developed technique is not only able to detect the shape of targets behind the concrete wall but also makes it rotational invariant.

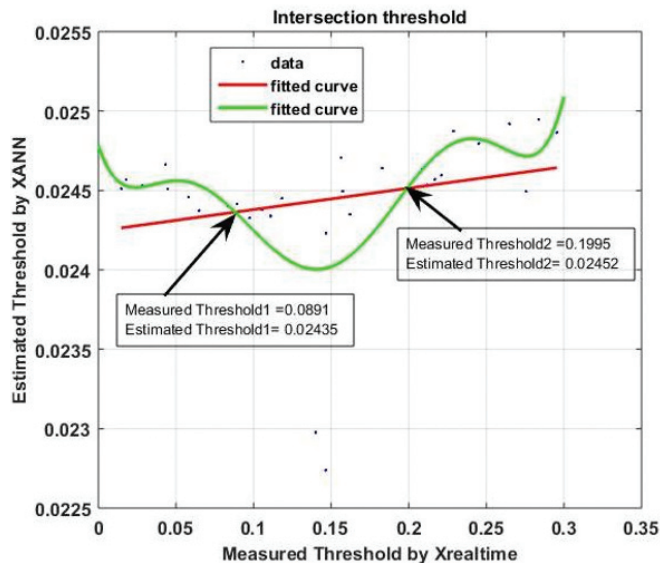


Figure 5. Curve fitting graph for X_{ANN} data and $X_{realtime}$ data.

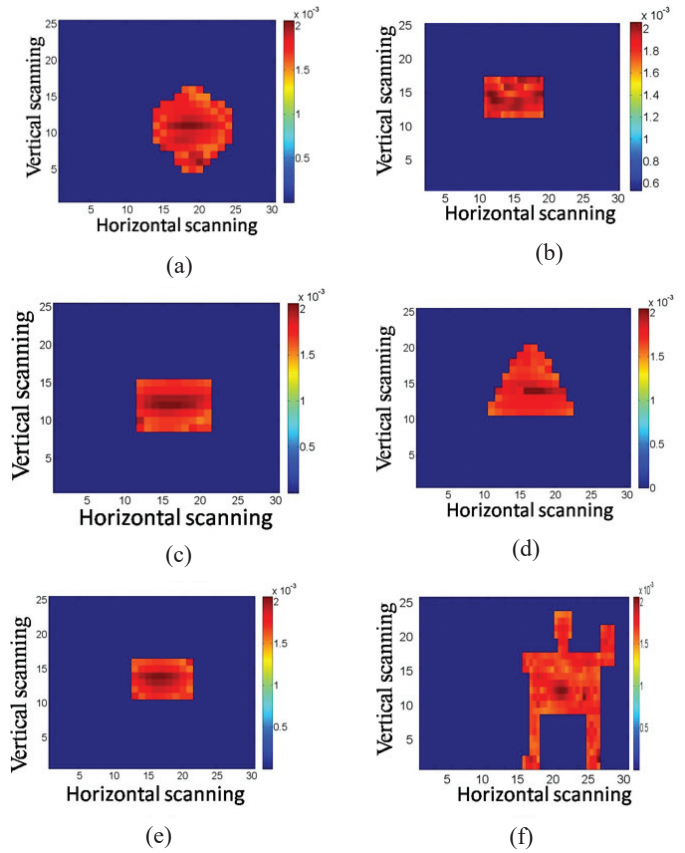


Figure 6. Threshold image of (a) Metal Circular target (b) Metal rectangular target (c) Tiles target (d) Metal Triangular targets (e) Wood square target and (f) Dummy metal man target.

Table 2. Final results of the image reconstructed using proposed technique

S. No.	Target ID	Raw image	Final image
1	MCT28		
2	MTT51		
3	TST88		
4	EST		

*MCT, MTT, TST, EST represent metal circular target, metal triangular target, tile square target, empty scene target respectively.

4. CONCLUSIONS

In the present paper, microwave imaging radar system based on SFCW mode has been used for data collection. C-Scan image has been generated by considering the maximum intensity point in range profile graph. This is called raw image, which is corrupted by noise and clutter due to variation in wall characteristics. Various image processing techniques such as windowing and back ground subtraction have been used for noise and clutter removal to obtain noise free image. Further, the raw image and noise free image has been used to train the neural networks. Threshold value has been selected by intersectional point of curve fit with the help of raw image data and trained ANN data. To validate the proposed techniques, real-time fresh TWI data has been taken, and correlated with trained ANN data. The shape of image has been generated by applying threshold point which has been selected by curve fitting method.

REFERENCES

- Logeswari, T. & Karnan, M. An improved implementation of brain tumor detection using segmentation based on soft computing. *J. Cancer Res. Exp.*, 2010, **2**(1), 006-014. doi: 10.5897/JCREO.9000002
- Khan, A. & Ansari, Z. Soft computing based medical image mining: a survey. *Int. J. Comput. Trends Technol.*, 2015, **27**(2), 76-79. doi: 10.14445/22312803/IJCTT-V27P113
- Liu, H. & Sato, M. In situ measurement of pavement thickness and dielectric permittivity by GPR using an antenna array. *NDTE Int.*, 2014, **64**, 65-71. doi: 10.1016/j.ndteint.2014.03.001
- Wei, X. & Zhang, Y. Autofocusing techniques for GPR data from RC bridge decks. *IEEE J. Sel. Top Appl. Earth Obs. Remote Sens.*, 2014, **7**(12), 4860-4868. doi: 10.1109/JSTARS.2014.2321710
- Seyfried, D.; Busche, A.; Janning, R.; Schmidt-Thieme, L. & Schoebel, J. Information extraction from ultrawideband ground penetrating radar data: a machine learning approach. In 2012 the 7th German Microwave Conference, 2012, 1-4.
- Seyfried, D.; Jansen, R. & Schoebel, J. Shielded loaded bowtie antenna incorporating the presence of paving structure for improved GPR pipe detection. *J. Appl. Geophys.*, 2014, **111**, 289-298. doi: 10.1016/j.jappgeo.2014.10.019
- Qi, F.; Liang, F.; Lv, H.; Li, C.; Chen, F. & Wang, J. Detection and classification of finer-grained human activities based on stepped-frequency continuous-wave through-wall radar. *Sensors*, 2106, **16**(6), 1-17. doi: 10.3390/s16060885
- Lu, B.; Song, Q.; Zhou, Z. & Wang, H. A SFCW radar for through wall imaging and motion detection. In 2011 8th European Radar Conference, Manchester, UK 2011, 325-328. <https://ieeexplore.ieee.org/abstract/document/6101000>.
- Liu, Y.; Meng, H.; Zhang, H. & Wang, X. Motion compensation of moving targets for high range resolution stepped-frequency radar. *Sensors*, 2008, **8**(5), 3429-3437. doi: 10.3390/s8053429
- Zhang, B. & Zhu, G. High frame rate stepped frequency through-wall imaging radar. In 2015 IEEE International Wireless Symposium (IWS 2015), Shenzhen, China, March 2015, 1-4. doi: 10.1109/IEEE-IWS.2015.7164612
- Mercuri, M.; Schreurs, D. & Leroux, P. SFCW microwave radar for in-door fall detection. In 2012 IEEE Topical Conference on Biomedical Wireless Technologies, Networks, and Sensing Systems (BioWireless), Santa Clara, CA, USA, January 2012, 53-56. doi: 10.1109/BioWireless.2012.6172729
- Marimuthu, J.; Bialkowski, K.S. & Abbosh, A.M. Stepped frequency continuous wave software defined radar for medical imaging. In 2014 IEEE Antennas and Propagation Society International Symposium (APSURSI), Memphis, TN, USA, July 2014, 1909-1910. doi: 10.1109/APS.2014.6905281
- Hartikainen, A.; Pellinen, T.; Huuskonen-Snicker, E. & Eskelinen, P. Algorithm to process the stepped frequency radar signal for a thin road surface application. *Constr. Build Mater.*, 2018, **158**, 1090-1098. doi: 10.1016/j.conbuildmat.2017.10.075
- Mohana, M.A.; Abbas, A.M.; Gomaa, M.L. & Ebrahim, S.M. Discrimination between landmine and mine-like targets using wavelets and spectral analysis. *NRIAG J. Astron. Geophys.*, 2013, **2**(1), 54-66. doi: 10.1016/j.nrjag.2013.06.009
- Zhang, H.; Ouyang, S.; Wang, G.; Wu, S. & Zhang, F. Dielectric spectrum feature vector extraction algorithm of ground penetrating radar signal in frequency bands. *IEEE Geosci. Remote. Sens. Lett.*, 2014, **12**(5), 958-962. doi: 10.1109/LGRS.2014.2369523
- Zhang, Y.; Venkatachalam A.S; Huston D & Xia T. Advanced signal processing method for ground penetrating radar feature detection and enhancement. *Proc. SPIE*, 2014, 9063, 906318. doi: 10.1117/12.2046338
- Temlioglu, E. & I. Erer. Clutter removal in ground-penetrating radar images using morphological component analysis. *IEEE Geosci. Remote. Sens. Lett.*, 2016, **13**(12), 1802-1806. doi: 10.1109/LGRS.2016.2612582
- Agarwal, S. & Kumar, B. SVM based concealed target quality monitoring system using millimeter wave radar. In 2016 11th International Conference on Industrial and Information Systems (ICIIS), 2016, 915-919. doi: 10.1109/ICIINFS.2016.8263069
- Gu, J.; Wang, Z.; Kuen, J.; Ma, L.; Shahroudy, A.; Shuai, B.; Liu, T.; Wang, X.; Wang, G.; Cai, J. & Chen, T. Recent advances in convolutional neural networks. *Pattern Recognit.*, 2018, **77**, 354-377. doi: 10.1016/j.patcog.2017.10.013
- Cai, J.L.; Tong, C.M. & Ji, W.J. Hybrid multi-phased particle swarm optimization for through-wall shape reconstruction and wall parameters estimation. *Prog. Electromagn. Res.*, 2013, **46**, 23-40.

- doi:10.2528/PIERB12091004
21. Dehmollaian, M. Through-wall shape reconstruction and wall parameters estimation using differential evolution. *IEEE Geosci. Remote. Sens. Lett.*, 2010, **8**, 201-205. doi: 10.1109/LGRS.2010.2056912
 22. Tekeli, B.; Gurbuz, S.Z. & Yuksel, M. Information-theoretic feature selection for human micro-Doppler signature classification. *IEEE Trans. Geosci. Remote Sens.*, 2016, **54**(5), 2749–2762. doi:10.1109/TGRS.2015.2505409
 23. Karabacak, C.; Gurbuz, S.Z.; Gurbuz, A.C.; Guldogan, M.B.; Hendeby, G. & Gustafsson, F. Knowledge exploitation for human micro-Doppler classification. *IEEE Geosci. Remote. Sens. Lett.*, 2015, **12**(10), 2125–2129. doi: 10.1109/LGRS.2015.2452311
 24. Wu, S.; Tan, K.; Xia, Z.; Chen, J.; Meng, S. & Guangyou, F. Improved human respiration detection method via ultra-wideband radar in through-wall or other similar conditions. *IET Radar, Sonar Navig.*, 2016, **10**(3), 468–476. doi: 10.1049/iet-rsn.2015.0159
 25. Sadeghi, S.; Mohammadpour-Aghdam, K.; Ren, K.; Faraji-Dana, R. & Burkholder, R. J. A. Pole-Extraction Algorithm for Wall Characterization in Through-the-Wall Imaging Systems. *IEEE Trans. Antennas Propag.*, 2019, **67**(11), 7106-7113. doi: 10.1109/TAP.2019.2927870
 26. Singh, A.P.; Dwivedi, S. & Jain, P.K. A novel application of artificial neural network for recognition of target behind the wall. *Microw. Opt. Technol. Lett.*, 2020, **62**(1), 152-167. doi: 10.1002/mop.32020
 27. Wan, Y.; Yu, C.Y.; Sun, C.H. & Chiu, C.C. The reconstruction of time domain through-wall imaging for a metallic cylinder. *Imaging Sci. J.*, 2015, **63**(2), 81-84. doi:10.1179/1743131X14Y.00000000084
 28. Wu, S.; Xu, Y.; Chen, J.; Meng, S.; Fang, G. & Yin, H. Through-wall shape estimation based on UWB-SP radar. *IEEE Geosci. Remote. Sens. Lett.* 2013, **10**(5), 1234-1238. doi: 10.1109/LGRS.2012.2237012
 29. Bivalkar, M. K.; Kumar, B. & Singh, D. Modified Low Rank Approximation for Detection of Weak Target by Noise space Exploitation in Through Wall Imaging. *Def. Sci. J.*, 2019, **69**(5), 464-468. doi: 10.14429/dsj.69.14952
 30. Agarwal, S.; Bisht, A.S.; Singh, D. & Pathak, N. P. A novel neural network based image reconstruction model with scale and rotation invariance for target identification and classification for Active millimetre wave imaging. *J. Infrared Millim. Terahertz Waves*, 2014, **35**(12), 1045–1067. doi: 10.1007/s10762-014-0109-5
 31. Sharma, P.; Kumar, B. & Singh, D. Development of Adaptive Threshold and Data Smoothing Algorithm for GPR Imaging. *Def. Sci. J.*, 2018, **68**(3), 316-325. doi: 10.14429/dsj.68.12354
 32. Kumar, B.; Upadhyay, R. & Singh, D. Development of an adaptive approach for identification of targets (match box, pocket diary and cigarette box) under the cloth with MMW imaging system. *Prog. Electromagn. Res.*, 2017, **77**, 37-55. doi:10.2528/PIERB17040804

CONTRIBUTORS

Mr Sandeep Kaushal did BE (Electronics) from North Maharashtra University, Maharashtra. He registered for PhD in Uttarakhand Technical University, Dehradun in the year 2010. His research interests include optical fiber communication, biomedical image processing, wireless technologies and microwave radar technology & applications. He has published more than 40 publications of research articles in various conferences and journals. At present, he is working as Associate Professor in the Department of ECE at ACET, Amritsar (Punjab), India. Real time data collection for concealed targets detection shape identification using the TWI system has been carried by the author.

Dr Bambam Kumar is currently working as assistant professor in NIT Patna. He has completed his PhD degree from the Indian Institute of Technology Roorkee (IIT Roorkee), Roorkee, India. He possesses more than 8 years of experience in teaching. He has got a young scientist award 2016 organised by UCOST, Uttarakhand. His research interest includes RF and microwave engineering, microwave and MMW imaging, and electromagnetic. The experimental study of shape identification using the TWI system has been carried out by the author.

Dr Prabhat Sharma received his BE from Govt. Engineering College Kota (Rajasthan Technical University, Kota) in 2000 and received his MTech in Integrated Electronics and Circuits from the Indian Institute of Technology, Delhi in 2011. Presently, he is working as a scientist in Instrument Research and Development Establishment, Dehradun and completed his PhD in the Department of Electronics and Communication Engineering at Indian Institute of Technology, Roorkee. His research interests include: RF Signal Processing, Remote sensing and Laser range sensor. The experimental study of shape identification using the TWI system has been carried out by the author.

Dr Dharmendra Singh received the PhD in electronics engineering from Banaras Hindu University, Varanasi, India. He has more than 25 years of experience in teaching and research. He is currently a Professor with the Department of Electronics and Communication Engineering, Indian Institute of Technology Roorkee, Roorkee, India. He has published more than 300 papers in various national/ international journals and conferences. His main research interests include microwave remote sensing, electromagnetic wave interaction with various media, polarimetric and interferometric applications of microwave data, numerical modelling, ground penetrating radar, and through-wall imaging.

In the current study he is headed by the author and the shape identification using the TWI system has been carried out under his supervision and guidance.